RAPID COMMUNICATIONS

PHYSICAL REVIEW B VOLUME 48, NUMBER 5 1 AUGUST 1993-I

# Langevin-dynamics study of nuclear relaxation to vortices in a layered superconductor

D. Reefman and H. B. Brom
*Kamerlingh Onnes Laboratory, Leiden University, P.O. Box 9506, 2300 RA Leiden, The Netherlands*
(Received 6 May 1993)

We have investigated the possibility of nuclear relaxation due to the magnetic field fluctuations induced by thermal motion of (pancake) vortices in a layered superconductor with a Langevin dynamics method. Only magnetic interactions between layers were taken into account. We found that for low fields the vortex lattice (VL) is rigid and hardly affects the relaxation time $T_1$. At higher vortex densities, for fields actually used in experimental NMR studies, effects may be visible. At the melting temperature of the VL a peak in the relaxation rate is observed.

Since the discovery of the high-$T_c$ cuprate superconductors, the understanding of the underlying mechanism of this phenomenon has been a major challenge. Because of its sensitivity to the electronic properties of a material, NMR measurements constitute a crucial test for any theory on superconductivity. As regards the high-$T_c$ materials, its sensitivity to antiferromagnetic (AF) fluctuations makes it also a valuable tool for the investigation of AF correlations in the normal state of these materials.

Up until now, mainly the importance of the vortex lattice (induced by the applied main field) with respect to the NMR line broadening has been studied extensively.[1–4] In Refs. 5 and 6 a significant field dependence of the relaxation rate in $YBa_2Cu_3O_7$ was observed, and the authors suggested that this could be due to the presence of the normal cores of vortices. In particular the fact that the measured effect depends linearly on the applied field supports this hypothesis (the number of normal cores is proportional to the applied field).[8] A problem, however, is the field effect at low temperatures, where the vortex lattice (VL) is pinned, and only a small fraction [of the order of $(\xi/a_0)^2$, $\xi$ is the coherence length, $a_0$ the vortex lattice parameter] of the nuclei can relax to the normal core. Though the large London penetration depth $\lambda_L$ creates the possibility of spin diffusion, this mechanism is likely to be inefficient.[7]

Especially in the highly anisotropic superconductors like, e.g., $Tl_2Ba_2CaCu_2O_8$, another relaxation channel may be of importance. In these materials, the vortex lattice is subject to large thermal fluctuations, which in turn result in magnetic field fluctuations. This vortex-induced spectral density can cause relaxation of the nuclei, and, because it is plausible that this relaxation mechanism is also proportional to the number of vortices, is probably linear in the applied field too.

Therefore, it is interesting to numerically simulate a system consisting of a stack of layers, each layer occupied by the same number of pancake vortices. As a first approximation, the Josephson interaction between the layers is neglected, and only magnetic interaction between the layers is taken into account. This approximation is not valid for the $YBa_2Cu_3O_7$ systems. Also pinning is not considered in this approach. Nevertheless, we think the outcome to be relevant for materials like the Bi- and Tl-based superconductors, due to the extreme anisotropy in these materials (with an anisotropy ratio $\Gamma > 5 \times 10^4$).[9] The simulations may also be of importance to the organic superconductors, e.g., $(BEDT\text{-}TTF)_2Cu(NCS)_2$,[10,11] which are known to be highly anisotropic (quasi-two-dimensional) superconductors.

The Langevin dynamics (LD) method used enables us to watch the system evolving in time, which in turn offers the possibility to calculate various time-dependent correlation functions needed for, e.g., the calculation of the NMR relaxation rates. In the following, we will focus in particular on the spin-lattice relaxation rate $T_1^{-1}$.

Our calculations are based on the model developed by Clem[12] (and subsequently repeated and extended by other authors[13,14]). The system under consideration consists of a stack of superconducting planes of thickness $d$, separated by a distance $s$. Only the magnetic interaction is taken into account. The supercurrent distribution in a layer due to a single pancake vortex in that layer is given by[12]

$$j_\phi(\rho, z=0) = \frac{\phi_0}{\pi\mu_0\Lambda(T)\rho}\left\{1 - \frac{\lambda_\parallel}{\Lambda}(1 - e^{-\rho/\lambda_\parallel})\right\}. \quad (1)$$

The supercurrent due to the same vortex in other layers is given by

$$j_\phi(\rho, z \neq 0) = -\frac{\phi_0\lambda_\parallel}{\pi\mu_0\Lambda^2(T)\rho}\left\{e^{-|z_n|/\lambda_\parallel} - e^{-r_n/\lambda_\parallel}\right\}, \quad (2)$$

where we have used cylindrical coordinates, and $r = \sqrt{\rho^2 + z_n^2}$. $z_n$ is the $z$ coordinate of the $n$th layer. $\Lambda = 2\lambda_L^2/d$, with $\lambda_L$ the bulk London penetration depth, and $\lambda_\parallel = \sqrt{s/d}\lambda_L$. $\Lambda$ is a "screening" length for the supercurrent in the central plane, whereas $\lambda_\parallel$ is the screening length of the supercurrent of the same vortex in different layers. If the current in the central layer is clockwise, the current induced in the other layers is counterclockwise. This results in a net, but weak, attraction for two pancake vortices in different layers, and a strong repulsion for two vortices in the same layer. The magnetic field components for a single pancake vortex are[12]

$$b_z(\rho, z) = \frac{\phi_0}{2\pi\Lambda(T)r}e^{-r/\lambda_\parallel},$$

$$b_\rho(\rho, z) = \frac{\phi_0}{2\pi\Lambda(T)\rho}\left\{\frac{z}{|z|}e^{-|z|/\lambda_\parallel} - \frac{z}{r}e^{-r/\lambda_\parallel}\right\}, \quad (3)$$

 

valid for all values of $z$.

We write the local nuclear Hamiltonian as $\mathcal{H}_n(\mathbf{r}) = \gamma_N \hbar \mathbf{B}(\mathbf{r}) \cdot \mathbf{I}$, which describes the coupling of the nucleus with spin $\mathbf{I}$ to the local internal field (induced by the vortices). $\gamma_N$ is the nuclear gyromagnetic ratio. The relaxation times can be written as[15,16]

$$\frac{1}{T_1} = 2J^{(1)}(\omega_I); \quad \frac{1}{T_2} = J^{(1)}(\omega_I) + \frac{1}{2}J^{(0)}(0), \qquad (4)$$

which is valid in the case in which the frequency with which $B$ fluctuates is much faster than the splitting that the fluctuations in $B$ would induce. The $J^{(n)}$ are the spectral densities of the magnetic fluctuations parallel to the applied field ($n = 0$) and perpendicular to it ($n = 1$):

$$J^{(0)}(\omega) = (\gamma_N \hbar)^2 \int_{-\infty}^{\infty} \langle B_z(\mathbf{r},0) B_z(\mathbf{r},\tau)\rangle_{\mathbf{r}} e^{-i\omega\tau} d\tau,$$

$$J^{(1)}(\omega) = \frac{1}{4}(\gamma_N \hbar)^2 \int_{-\infty}^{\infty} \langle B_+(\mathbf{r},0) B_-(\mathbf{r},\tau)\rangle_{\mathbf{r}} e^{-i\omega\tau} d\tau. \quad (5)$$

$\langle\rangle_{\mathbf{r}}$ represents an ensemble average. $B_\pm$ is defined as $B_\pm = B_x \pm iB_y$.

In the simulation, we keep track of the time-dependent field correlation function $\langle B(\mathbf{r},0)B(\mathbf{r},\tau)\rangle_{\mathbf{r}}$, for all needed components of $\mathbf{B}$, and calculate the Fourier transform afterwards. To correct for the time-independent induction due to the vortices, one can take the $J^{(0)}(0)$ value from an extrapolation to zero from low, but nonzero, frequencies, which corresponds to replacing $\mathbf{B}$ by its deviation $\delta\mathbf{B}$ from the average value. In calculating $T_1$, we will set $\gamma_N$ equal to $\gamma_H$, the gyromagnetic ratio for a proton.

In the large-$\kappa$ (London) limit, we can treat the vortices as classical, massless particles, moving in a continuous medium with viscosity $\eta$. The equations of motion for a set of $M$ vortices are then given by

$$\eta \mathbf{v}_i(t) = \mathbf{F}_v + \mathbf{R}_i(t) \quad i = \{1, ..., M\}. \qquad (6)$$

Here $\mathbf{F}_v$ denotes the force resulting from the actions of all vortices. The potential originating from pinning centers is neglected in the present simulation.

The force $\mathbf{f}$ between two vortices separated by a distance $\mathbf{r}$ is written as $\mathbf{f}(\mathbf{r}) = \mathbf{j}(\mathbf{r}) \times \boldsymbol{\phi}_0$. In the present case, $\boldsymbol{\phi}_0$ is always parallel to the $z$ axis (no Josephson coupling), which substantially simplifies the interaction. $\eta$ is a friction coefficient, given within the framework of the Bardeen-Stephen model.[17] $\mathbf{R}(t)$ is a random force corresponding to a temperature $T$ as defined by the fluctuation dissipation theorem.[18]

The set of differential equations in Eq. (6) is solved with an LD algorithm (see Ref. 2 for a detailed description of the method). Due to the long-range $1/r$ interaction between the vortices, a problem arises in real-time simulations because of the periodic boundary conditions that should be imposed on the system. We therefore introduce an effective force $\mathbf{F}$ that a vortex exerts on another vortex in a repeated system of size $L_x \times L_y$: $\mathbf{F}(\mathbf{r}) = \sum_{ij} \mathbf{f}(\mathbf{r} - iL_x\mathbf{u}_x - jL_y\mathbf{u}_y)$. One of the above summations can be carried out analytically. The resulting summation is done numerically, and converges very fast.

In all simulations, the vortices were placed at their ideal lattice positions at $t = 0$. The time step $\Delta t$ used did not result in any displacement of more than $0.05a_0$ during the simulation. It was checked that the results of the simulation did not change significantly on halving the time step. This gave us confidence that the integration time is closely related to the real time. For each temperature, a single run consisted of at least 50000 time steps.

During the simulation, we also calculated, besides the field correlation functions, $g_0(t) = \langle|\boldsymbol{\rho}(z,t) - \boldsymbol{\rho}(z,0)|^2\rangle$ needed for evaluating the diffusion coefficient.

In our simulations, we have taken parameters that are believed to be representative for the Bi- and Tl-based superconductors: $\lambda_\parallel = 1400$ Å and $T_c(B = 0) = 90$ K. The temperature dependence of the penetration depth was taken from Ref. 19, and $\eta$ was extracted from data in Ref. 20. With the appropriate scaling of $T_c$, these parameters are also reasonable for the highly anisotropic organic superconductors, e.g., $(BEDT\text{-}TTF)_2Cu(NCS)_2$. All simulations were done on $168 \times 15$ lattices ($\frac{N_z s}{\lambda_\parallel} \approx 0.2, L_x \approx L_y \approx 13a_0$), and a few checks for finite size effects were made on $418 \times 10$ lattices ($\frac{N_z s}{\lambda_\parallel} \approx 0.13, L_x \approx L_y \approx 20a_0$).

We now turn to the results. In the low-field regime, one expects that the vortices are separated by such a large distance, that the vortex pancakes more or less behave like ordinary three-dimensional (3D) London vortices for temperatures which are not too close to $T_c$. In fact, this means that first of all the layer decoupling temperature $T_d$ is very close to the lattice melting temperature $T_m$ (or does not even exist), because the distance between vortices in the same layer is proportional to $1/\sqrt{B}$, whereas the distance between vortices in different layers is constant ($s$). Second, the melting temperature should be only slightly less than $T_c$, because the energy to produce a dislocation for a single (rigid) flux line is proportional to its length, and melting will be due to the divergence of the London penetration depth $\lambda_L$ near $T_c$. Indeed, for the lowest field numerically accessible (0.01 T), we found for the layer decoupling temperature $T_d/T_c \approx 0.85$, and for the melting temperature of the resulting quasi-2D VL $T_m/T_c \approx 0.97$.

At $T_m$, the in-plane diffusion constant $D_{\rm ip}$, defined as $D_{\rm ip} = \lim_{t\to\infty} \frac{d}{dt} g_0(t) - \tilde{D}$, rises abruptly. Here the term $\tilde{D}$ is the correction for the motion of the vortices in a plane as a whole (this correction is necessary, because the vortices in a certain layer may have a common drift with respect to the vortices in a different layer). This change of $D_{\rm ip}$ is accompanied by a drastic decrease of the positional correlation length $\xi(T)$. The spectral density $J^{(1)}(\omega)$ slightly increases on increasing temperature, and drops below $T_d$.

We should remark, however, that the values which we obtained for $J^{(1)}(\omega)$ are not easily accessible in an actual NMR experiment. Reasonable NMR frequencies are higher than 5 MHz, and at this frequency the obtained value for $T_1^{-1}$ is of the order of $10^{-3}$ s$^{-1}$ for a $^1$H nucleus. At higher frequencies, the rate is even slower. Competing relaxation channels, like, e.g., *via* the dipolar coupling,

usually result in relaxation times which are at least an order of magnitude shorter, and will thus dominate the effect of relaxation to vortices.

For higher fields ($B = 1$ T) the decoupling of the layers occurs at a much lower temperature: $T_d \approx 0.005T_c$. At these low temperatures, the in-plane diffusion is still zero, as can be inferred from the inset in Fig. 1. At $T_m$, about $0.55T_c$, $D_{\rm ip}$ features a small jump, and increases rapidly with temperature. (It turns out, that $D_{\rm ip}$ is hardly sensible to the lattice size; for $T = 0.1T_c$ the coefficients obtained for the larger and smaller lattices differ by about 10%.) At $T_m$ the correlation length in the $z$ direction shows a sudden drop (from about four layers to two layers), though the layers are decoupled already.

In Fig. 1 we depict the temperature dependence of $1/T_1 = 2J^{(1)}(\omega)$ for a proton at fixed frequencies of 10, 30, and 70 MHz. Clearly, there is a maximum in $J^{(1)}(\omega)$ at approximately $T \approx 0.6T_c$ for the lower frequencies, and at $T \approx 0.7T_c$ for 70 MHz. The height of the maximum decreases with increasing frequency. For frequencies higher than a cutoff frequency ($\sim$ 85 MHz), $J^{(1)}(\omega)$ is zero for all temperatures. This cutoff frequency is determined by the viscosity of the vortices, which tends to damp all high-frequency oscillations in the system.

An explanation for the observed maximum might be the following. For increasing temperatures, the thermal fluctuations of the vortices become more severe, and $J^{(1)}(\omega)$ will increase. At the melting temperature, the correlation of the vortices in the $z$ direction, which for lower temperatures was still substantial, breaks down, and the $xy$ fluctuations of the magnetic field start to average out more effectively, reducing $T_1^{-1}$.

The melting also influences $J^{(0)}(\omega)$, as can be inferred from the inset in Fig. 2; below $T_m$ $J^{(0)}(\omega)$ drops, corresponding to a reduction in transverse relaxation rate (but an increase in linewidth[2]).

In contrast with the low-field case, in high-field relaxation effects may be observable. Values for $T_1^{-1}$ obtained from $J^{(1)}(\omega)$ range between 0.1 and 1 $s^{-1}$, and are thus in the accessible range. In fact, the maximum in $T_1^{-1}$, which we predict at $T_m$, has been observed in the layered organic superconductor (BEDT-TTF)$_2$Cu(NCS)$_2$ (Refs. 10 and 11) at $T/T_c \approx 0.4$ ($T_c = 12$ K), which is also the VL melting temperature.[21] Also quantitatively, the calculated $T_1^{-1}$ compares well with experiment. The observed peak shifts to somewhat lower temperatures on increasing the frequency and, concomitantly, the field. We therefore have calculated also the field dependence of $J^{(1)}(\omega)$ for fixed temperatures (see Fig. 2). For the highest temperature ($T/T_c = 0.4$) the VL is molten for all fields larger than 2 T. Apparently, a higher vortex density (induced by a larger field) causes larger $B_{xy}$ fluctuations. For the largest field, the spectral density seems to level off; this is most strongly evidenced by the $J^{(1)}$(10 MHz)

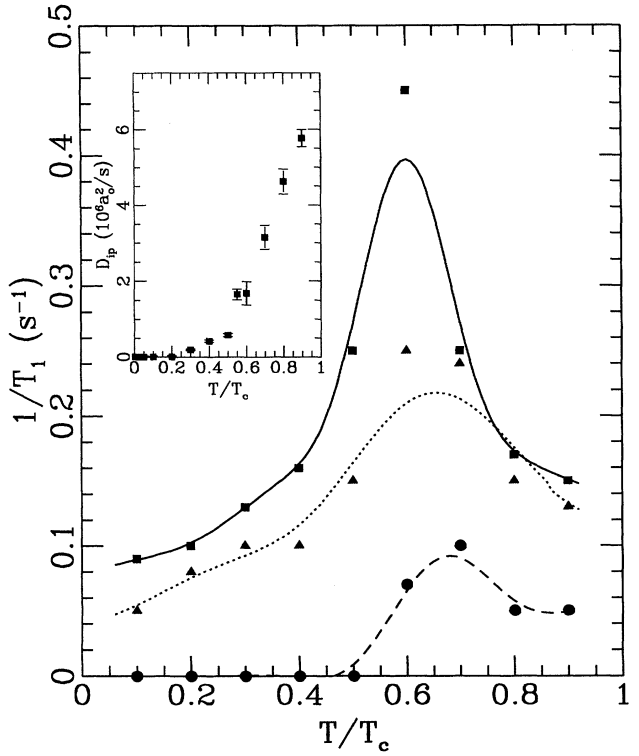


FIG. 1. Temperature dependence of $1/T_1[\propto J^{(1)}(\omega)]$ for a proton, in a field of 1 T, at fixed frequencies of 10 MHz (squares), 30 MHz (triangles), and 70 MHz (circles). The curves (drawn: 10 MHz, dotted: 30 MHz, dashed: 70 MHz) are guides to the eye. Inset: diffusion constant $D_{\rm ip}$ in a system of 15 layers in a field of 1 T.

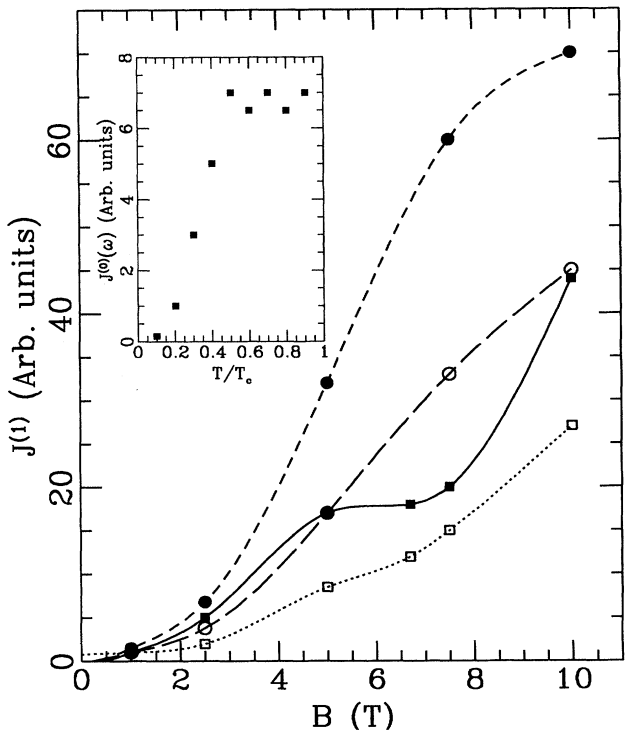


FIG. 2. Spectral density $J^{(1)}(\omega)$ as a function of field for a temperature of $0.2T_c$ (squares) and $0.4T_c$ (circles). Solid symbols are for $\omega = 10$ MHz, open symbols for $\omega = 30$ MHz. The curves are guides to the eye. Inset: spectral density $J^{(0)}(\omega)$, for high field (1 T) as a function of temperature at a fixed frequency of 10 MHz.

data (black circles). Due to the high vortex density, the $B_{xy}$ fluctuations start to average out, which explains why the effect is not so strong for the $J^{(1)}(30\ \mathrm{MHz})$ data, because for this frequency averaging should occur on a time scale which is three times shorter.

For $T = 0.2T_c$, the VL melts for a field in between 5 and 7.5 T. The plateau in $J^{(1)}(10\ \mathrm{MHz})$ may be related to the sudden drop in $\xi_z$ at $T_m$, which leads to strong averaging of the $B_{xy}$ fluctuations. Again, for a higher frequency $\omega$ this averaging is not as effective, explaining why the $J^{(1)}(30\ \mathrm{MHz})$ data are much less influenced by the melting.

A general feature is that larger fields lead to higher relaxation rates (at least for $B < 10$ T; $\omega < 70$ MHz). In this context, the curves in Fig. 1 should be rescaled appropriately, when compared to experiments on the same nucleus for different $\omega$ (and thus $B$). Also, $T_m$ shifts down for higher $B$, which causes the maxima in Fig. 1 to occur at lower $T$. Correcting the position of the peak in Fig. 1 for this effect, the calculated maximum shifts down on increasing $\omega$, as observed in (BEDT-TTF)$_2$Cu(NCS)$_2$.[10,11]

The values obtained for $T_2$ are somewhat smaller than those obtained for $T_1$; because the usual dipolar interaction gives rise to a more efficient relaxation pathway it is improbable that any clear $T_2$ effect due to the vortex lattice may be observed.

In summary, we have shown that thermal motion of the vortices induced by the applied field establishes a relaxation channel for the nuclei in an NMR experiment. It appears that the effects are most pronounced close to the VL melting temperature. The results obtained for (BEDT-TTF)$_2$Cu(NCS)$_2$ (Refs. 10 and 11) might well be interpreted in this way. At low temperatures, where $T_1$ is hardly frequency dependent, the increase of the applied field results in an almost linear increase of the rate $T_1^{-1}$. Relaxation to vortices becomes improbable for frequencies higher than some cutoff frequency $\omega_c$, which is expected to be about 85 MHz for a parameter set typical for the high-$T_c$ materials.

Although we used the quasi-two-dimensionality of the VL explicitly, we believe the results obtained below $T_m$ still to be relevant to Y-Ba-Cu-O. In our view, vortex dynamics is therefore an alternative explanation for the field dependence of the relaxation rate observed in Refs. 5 and 6.

The authors want to acknowledge P. H. Kes for a critical reading of the manuscript, and D. E. MacLaughlin for valuable discussions. This work was sponsored by the Stichting Nationale Computer Faciliteiten (National Computer Facilities Foundation) for the use of supercomputer facilities, with financial support from the Nederlandse Organisatie voor Wetenschappelijk Onderzoek.

[1] M. Mehring, F. Hentsch, H. Mattausch, and A. Simon, Solid State Commun. **75**, 753 (1990).
[2] D. Reefman and H. B. Brom, Physica C **183**, 212 (1991).
[3] H. B. Brom and H. Alloul, Physica C **177**, 297 (1991).
[4] P. Caretta and M. Corti, Phys. Rev. Lett. **68**, 1236 (1992).
[5] F. Borsa, A. Rigamonti, M. Corti, J. Ziolo, O.-B. Hyun, and D. Torgeson, Phys. Rev. Lett. **68**, 698 (1992).
[6] J. A. Martindale *et al.*, Phys. Rev. Lett. **68**, 702 (1992).
[7] A. Z. Genack and A. G. Redfield, Phys. Rev. Lett. **31**, 1204 (1973).
[8] D. E. MacLaughlin, in *Solid State Physics: Advances in Research and Applications*, edited by H. Ehrenreich, F. Seitz, and D. Turnbull (Academic, New York, 1976), Vol. 31.
[9] J. C. Martinez *et al.*, Phys. Rev. Lett. **69**, 2276 (1992).
[10] T. Takahashi, K. Kanoda, and G. Saito, Physica C **185-189**, 366 (1991).
[11] D. Schweitzer *et al.*, Synth. Met. **27**, A465 (1988).
[12] J. R. Clem, Phys. Rev. B **43**, 7837 (1991).
[13] K. H. Fisher, Physica C **178**, 161 (1991).
[14] Y. M. Ivanchenko, L. V. Belevtsov, Y. A. Genenko, and Y. V. Medvedev, Physica C **193**, 291 (1992).
[15] A. Abragam, *Principles of Nuclear Magnetism* (Oxford University Press, London, 1989).
[16] C. P. Slichter, *Principles of Magnetic Resonance*, 3rd edition (Springer-Verlag, Berlin, 1990).
[17] J. Bardeen and M. J. Stephen, Phys. Rev. **140**, A1197 (1965).
[18] L. E. Reichl, *A Modern Course in Statistical Physics* (Arnold, London, 1987).
[19] B. Rakvin, T. A. Mahl, A. S. Bhalla, Z. Z. Sheng, and N. S. Dalal, Phys. Rev. B **41**, 769 (1990).
[20] P. H. Kes, P. Berghuis, S. Q. Guo, C. F. J. Flipse, J. G. Lensink, and R. P. Griessen, J. Less-Common Met. **151**, 325 (1989).
[21] K. Murata *et al.*, Synth. Met. **27**, A341 (1988).